Table 3. Multivariate Analysis of Factors Independently Associated With Persistence of HBsAg Positivity Following Acute Hepatitis B

	Persistence of HBsAg More Than 6 Months From AHB		
Factors	Odds Ratio	95% CI	*P* Value
ALT (per 1 IU/L increase)	1.000	0.999-1.000	0.035
HBV DNA (per 1 log copy/mL increase)	1.176	0.931-1.484	0.173
Genotypes			
Non-A	1.00		
A	4.224	1.853-9.631	0.001

95% CI, 95% confidence interval; ALT, alanine aminotransferase; HBV, hepatitis B virus.

in the former group than in the latter group. The percentages of HBV genotype A (48.8% versus 88.9%, $P = 0.018$) and NAs treatment (+) (48.3% versus 88.9%, $P = 0.017$) were significantly higher among patients in whom the HBsAg persisted for more than 12 months.

Factors Independently Associated With Viral Persistence Following AHB. A stepwise logistic regression model was used to perform multivariate analysis which explains relationships between some factors and persistence of HBsAg positivity more than 6 months following AHB. Peak ALT level, peak HBV DNA level, genotype A, and treatment with NAs were retained in the final multivariate logistic model in a backward stepwise manner ($P < 0.1$). For predicting the persistence of HBsAg for more than 6 months, only genotype A was independently associated with progression of AHB to the persistence of HBsAg (odds ratio [OR]: 4.224, $P = 0.001$, Table 3).

Characteristics of Patients Who Progressed to Chronicity That Was Defined as the Persistence of HBsAg for More Than 12 Months Following Acute Hepatitis B. Table 4 shows the clinical and virological characteristics of nine patients who progressed to chronicity defined as the persistence of HBsAg for more than 12 months following AHB. Among the nine patients who progressed to chronicity from AHB, eight (88.9%) were men and eight (88.9%) were HBeAg-positive. In general, among the patients who progressed to chronicity following AHB, the peak HBV DNA levels were high, and the peak total bilirubin and ALT levels were low. In eight (88.9%) patients, entecavir was administered; however, the duration until the onset of NA treatment from AHB onset was long (75-570 days).

Early Onset of Treatment With NAs Was Able to Prevent Viral Persistence After AHB Caused by Genotype A. The cumulative proportion maintaining HBsAg positivity during follow-up, expressed in terms of time after AHB onset, were significantly longer in patients with NAs treatment than in those without NAs treatment ($P = 0.046$, Fig. 2A). Table 5 shows the percentages of patients in whom HBsAg persisted for more than 6 or 12 months among patients categorized based on the period of time (i.e., duration) until the onset of NAs treatment. For patients in whom the onset of NAs treatment was less than 4 weeks from the onset of AHB, 12.7% of the patients showed persistent HBsAg for more than 6 months, while none showed HBsAg positivity for more than 12 months. For patients in whom the onset of NAs treatment was at 5-8 weeks, 37.5% of the patients showed persistent HBsAg for more than 6 months, whereas none showed persistent HBsAg for more than 12 months. For all groups, the period of HBsAg positivity in patients starting NAs treatment within 8 weeks from AHB onset was significantly shorter than that in patients beginning NAs treatment after more than 8 weeks from AHB onset ($P < 0.0001$, Fig. 2B). Patients starting NAs treatment within 8 weeks from AHB onset never progressed to chronicity after AHB caused by genotype A.

Table 4. Characteristics of Patients Who Progressed to Chronicity Following Acute Hepatitis B

Case	Age	Gender	HIV	HBeAg	HBV DNA (log copies/mL)	Total Bilirubin (mg/dL)	ALT (IU/L)	Observation Period (Months)	NAs Treatment	Duration Until NAs Treatment (Days)	Transmission Routes	Genotype
1	23	Male	(−)	(+)	7.6	1.7	1271	26	ETV	570	Heterosexual	A
2	40	Male	(−)	(−)	8.8	1.4	568	13	ETV	240	Heterosexual	A
3	45	Male	(−)	(+)	7.7	0.9	867	57	ETV	135	Heterosexual	A
4	37	Male	(−)	(+)	7.6	3.4	384	29	ETV	75	Unknown	A
5	54	Male	(−)	(+)	9	2	455	17	ETV	155	Homosexual	A
6	45	Male	(−)	(+)	4.8	21.2	512	60	(−)	(−)	Homosexual	A
7	61	Male	(−)	(+)	9.1	1.5	804	17	ETV	88	Unknown	A
8	56	Male	(−)	(+)	9.0	1.1	1820	14	ETV	118	Unknown	A
9	31	Female	(−)	(+)	7.4	0.8	296	66	ETV	150	Blood transfusion	C

HIV, human immunodeficiency virus; HBeAg, hepatitis B e-antigen; HBV, hepatitis B virus; ALT, alanine aminotransferase; NAs, nucleotide analogs; ETV, entecavir.

Table 5. Proportion of Patients in Whom HBsAg Persisted for More Than 6 or 12 Months Among Patients Categorized Based on the Number of Weeks Until the Onset of NAs Treatment

Duration Until Onset of NAs Treatment (Weeks)	Persistence of HBsAg for More Than 6 Months	Persistence of HBsAg for More Than 12 Months	Total Patients
<4 weeks (n, %)	9 (12.7)	0 (0)	71
5-8 weeks (n, %)	6 (37.5)	0 (0)	16
9-12 weeks (n, %)	1 (33.3)	1 (33.3)	3
13-16 weeks (n, %)	4 (100)	1 (25.0)	4
>17 weeks (n, %)	9 (100)	6 (66.7)	9
Total	29	8	103

HBsAg, hepatitis B surface antigen; NAs, nucleotide analogs.

Discussion

A multicenter nationwide study was conducted throughout Japan to evaluate the influence of clinical and virological factors on chronic outcomes in Japanese patients who contracted AHB in adulthood. The study was feasible in Japan, where a universal vaccination program for HBV has not been implemented because of the extremely high efficacy of the immunoprophylaxis that is given to babies born to carrier mothers. The implementation of this program has resulted in a decrease in the persistent HBV carrier rate from 1.4% to 0.3%.[19] Selective vaccination means that Japanese are more likely to be infected with HBV by way of horizontal transmission since the percentage of the population possessing anti-HBs is much lower than that in countries in which universal vaccination programs have been established.[20] In addition, Japan is faced with the ever-increasing impacts of globalization: as many as 17 million Japanese travel abroad and over 7 million people visit Japan from overseas each year. This "population mixing" may help to explain the increased prevalence in Japan of AHB due to genotype A, which is transmitted through indiscriminate sexual contact. Consequently, Japan may be the only country in the world where the influences of HBV genotypes, including genotype A (as is predominant in Western countries) and genotypes B and C (as are predominant in Asian countries), on chronic outcomes after AHB can be compared.

Currently, the persistence of HBsAg in serum for more than 6 months is considered to represent a progression to chronic infection.[21] However, our data showed that HBsAg frequently disappeared between 7 to 12 months after the onset of AHB in patients with genotype A (31/107 [29.0%]) and non-A genotypes (9/105 [8.6%]) (Fig. 1). These patients were considered to exhibit prolonged cases of AHB, rather than persistent infection. This finding reflects the higher sensitivity of the most up-to-date assays for HBsAg as compared with previous methods. In the present study, HBsAg was measured by CLIA, which has been reported to be about 150 times more sensitive in the detection of HBsAg than reverse passive hemagglutination (RPHA)-HBsAg, which has been used for the last 30 years in Japan.[22] The use of a more sensitive assay for HBsAg results in a longer period during which HBsAg may be detected. In this study, HBsAg did not disappear in nine patients after remaining continuously detectable for more than 12 months. Therefore, the persistence of HBsAg for more than 12 months, as measured with a highly sensitive method for detecting HBsAg, may be suitable for defining the progression of AHB to chronicity; however, further study is necessary to determine whether this definition is appropriate worldwide.

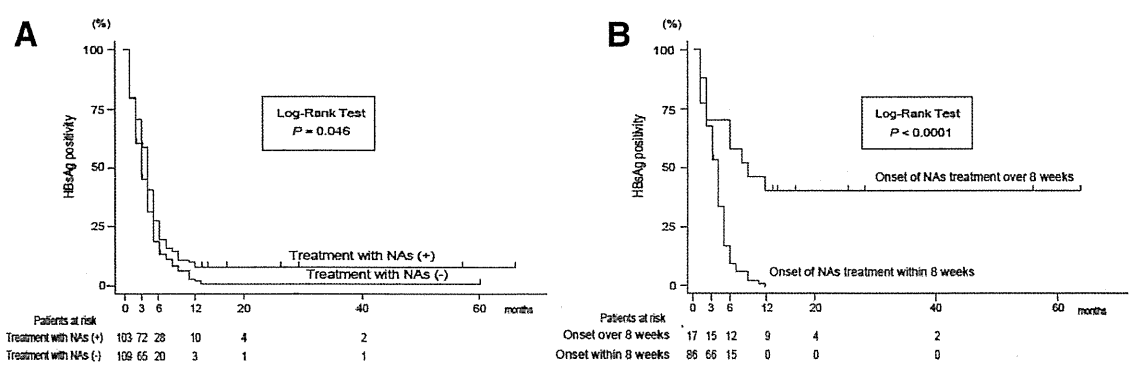

Fig. 2. (A) Comparison of the cumulative proportion of AHB patients maintaining HBsAg positivity between treatment with NAs (+) and treatment with NAs (−), as analyzed using the Kaplan-Meier test. $P = 0.046$, treatment with NAs (+): red line, treatment with NAs (−): blue line. (B) Comparison of the cumulative proportion of AHB patients in genotype A maintaining HBsAg positivity between treatment onset with NAs within 8 weeks and treatment onset with NAs over 8 weeks after onset of AHB, as analyzed using the Kaplan-Meier test. $P < 0.0001$, treatment onset with NAs over 8 weeks: red line, treatment onset with NAs within 8 weeks: blue line.

It has been reported that ~10% of patients who contract HBV as adults do not clear HBsAg from their serum and become carriers.[23] Meanwhile, a wide variation has been seen in the rate of persistence after AHB infection in adults. For example, viral persistence following AHB was seen in 0.2% (1/507) of adults in Greece,[24] 7.7% (5/65) of adult Alaskan Eskimos, and 12.1% (7/58) of adults in Germany.[25] The difference in the proportion of patients progressing from AHB to chronicity in different regions may be attributable to virological and host factors. In this study, 4.2% (9/212) of patients progressed to chronicity after AHB: 7.5% (8/107) of those infected with genotype A and 0.9% (1/105) of those infected with non-A genotypes. The non-A genotypes included genotypes B, C, D, F, and H (n = 25, 77, 1, 1, and 1, respectively). Genotypes B and C are predominant in eastern Asian countries, where the majority of those infected with HBV acquired the virus during the perinatal period by way of vertical transmission.[26] On the other hand, genotype A is predominant in Western countries, where the main route is horizontal transmission later in life.[26,27] Because HBeAg persists long after the infection in the genotype C as compared to other genotypes, this genotype has been shown to be a risk factor for perinatal and horizontal transmission in newborns and children.[28] The predominance of genotype A in Western countries may be attributable to a higher chronicity rate following AHB by way of horizontal transmission in adults.

In this study the characteristics of AHB associated with genotype A were a higher peak level of HBV DNA and a lower peak level of ALT. These findings were similar to those for patients with HBV-HIV coinfection.[29] Such characteristics of genotype A or coinfection with HIV are assumed to be attributable to milder hepatitis associated with weaker cellular immune responses. More slowly replicating viruses have been reported to evoke weaker cellular responses, enhancing the likelihood of persistence.[30] Indeed, our prior study showed that the replication of genotype A was significantly slower than that of genotype C in immunodeficient, human hepatocyte chimeric mice.[31] Moreover, variation among genotypes in the expression pattern of HBeAg may affect the progression of AHB to chronicity. Another previous study of ours revealed that a single form of HBeAg was detected by western blot analysis in serum samples from patients infected with genotypes B through D, but that two additional larger forms of HBeAg were detected in patients with genotype A.[32] Milich and Liang[33] reported that HBeAg may modulate the host immune response as a tolerogen to promote chronicity. Therefore, the different expression pattern of HBeAg by genotype A HBV may contribute to chronicity following AHB.

Early NAs initiation appeared to enhance the viral clearance across genotypes, although treatment with NAs did not show any overall benefit in duration of HBsAg. Previous studies examining the efficacies of NAs for preventing progression to chronic infection after AHB have reported conflicting results. Some small-scale studies have suggested the efficacy of lamivudine and entecavir in preventing the progression of AHB to chronic hepatitis.[34,35] Another study showed a lower seroconversion rate of HBsAg in lamivudine users.[36] Further, a randomized placebo-controlled trial showed no significant difference in clinical outcomes.[37] However, these previous studies did not mention the prevalence of HBV genotypes in the respective study populations. Although this was a retrospective study, our study included data on the prevalence of HBV genotypes. Additionally, our findings suggested that larger prospective randomized studies for every HBV genotype should be performed to determine whether early treatment with NAs prevented the progression of AHB to a chronic state.

In conclusion, in Japan genotype A was an independent risk factor for progression to chronic infection following AHB in adults. Confirmation of this association in patients with AHB in other countries is desirable and may provide insight into the pathogenetic mechanisms underlying this association. Early NA treatment appeared to reduce the likelihood of chronicity but this potentially important intervention needs to be prospectively studied before recommendations can be made.

Appendix

Members of the Japanese AHB Study Group include Yasuharu Imai (Ikeda Municipal Hospital), Norie Yamada, Hideaki Takahashi (St. Marianna University School of Medicine), Koji Ishii (Toho University School of Medicine), Hideyuki Nomura (Shin-Kokura Hospital), Jiro Nishida (Tokyo Dental Collage Ichikawa General Hospital), Shigeru Mikami (Kikkoman Hospital), Tsuneo Kitamura (Juntendo University Urayasu Hospital), Akihito Tsubota (Kashiwa Hospital Jikei University School of Medicine), Noritomo Shimada (Shinmatsudo Central General Hospital), Tetsuya Ishikawa (Nagoya University Graduate School of Medicine), Yoshiyuki Ueno (Tohoku University Graduate School of Medicine), Tomoyoshi Ohno (Social Insurance Chukyo Hospital), Etsuro Orito (Nagoya

Daini Red Cross Hospital), Michihiro Suzuki (Kawasaki Municipal Tama Hospital), Hitoshi Takagi (Gunma University Graduate School of Medicine), Eiichi Tomita (Gifu Municipal Hospital), Kumada Takashi (Ogaki Municipal Hospital), Toshihiko Mizuta (Saga University Faculty of Medicine), Tetsuya Mine (Tokai University School of Medicine), Jong-Hon Kang (Teine-Keijinkai Hospital), Katsuji Hirano (Juntendo University Shizuoka Hospital), Hirohito Tsubouchi (Kagoshima University Graduate School of Medical and Dental Sciences), Akito Nozaki (Yokohama City University Medical Center), Akito Sakai (Kanazawa University Graduate School of Medical Science), Shuhei Nishiguchi (Hyogo College of Medicine), Akihiro Tamori (Osaka City University Graduate School of Medicine), Satoru Hagiwara (Kinki University School of Medicine), Takahide Nakazawa (University of Kitasato East Hospital), Michio Sata (Kurume University School of Medicine), Toshiro Kamoshida (Hitachi General Hospital) Atsushi Takahashi (Fukushima Medical University School of Medicine), Satoshi Kakizaki (Gunma University Graduate School of Medicine), Yoshimasa Kobayashi (Hamamatsu University School of Medicine), Shigeru Sasaki (Sapporo Medical University), Tadashi Ikegami (Tokyo Medical University Ibaraki Medical Center), Yoichi Hiasa (Ehime University Graduate School of Medicine), Kenji Nagata (University of Miyazaki), Tomoyuki Kubota (Saiseikai Niigata Daini Hospital), Hiroshi Mitsui (Tokyo Teishin Hospital), Norihiko Yamamoto (Mie University School of Medicine), Masataka Tsuge (Hiroshima University), Shuichi Sato (Shimane University Hospital), Yoshito Ito (Kyoto Prefectural University of Medicine), Wataru Sato (Akita University School of Medicine), Shigeharu Uchida (Japanese Red Cross Society), Yuki Tada (National Institute of Infectious Diseases), Toshiaki Mizuochi (National Institute of Infectious Diseases), Norihiro Furusho (Kyushu University), and Shuhei Hige (Hokkaido University Graduate School of Medicine).

References

1. Mast EE, Alter MJ, Margolis HS. Strategies to prevent and control hepatitis B and C virus infections: a global perspective. Vaccine 1999; 17:1730-1733.
2. Lavanchy D. Worldwide epidemiology of HBV infection, disease burden, and vaccine prevention. J Clin Virol 2005;34(Suppl 1):S1-S3.
3. Okamoto H, Tsuda F, Sakugawa H, Sastrosoewignjo RI, Imai M, Miyakawa Y, et al. Typing hepatitis B virus by homology in nucleotide sequence: comparison of surface antigen subtypes. J Gen Virol 1988; 69(Pt 10):2575-2583.
4. Norder H, Hammas B, Lofdahl S, Courouce AM, Magnius LO. Comparison of the amino acid sequences of nine different serotypes of hepatitis B surface antigen and genomic classification of the corresponding hepatitis B virus strains. J Gen Virol 1992;73(Pt 5):1201-1208.
5. Miyakawa Y, Mizokami M. Classifying hepatitis B virus genotypes. Intervirology 2003;46:329-338.
6. Fung SK, Lok AS. Hepatitis B virus genotypes: do they play a role in the outcome of HBV infection? HEPATOLOGY 2004;40:790-792.
7. Norder H, Courouce AM, Coursaget P, Echevarria JM, Lee SD, Mushahwar IK, et al. Genetic diversity of hepatitis B virus strains derived worldwide: genotypes, subgenotypes, and HBsAg subtypes. Intervirology 2004;47:289-309.
8. Kurbanov F, Tanaka Y, Mizokami M. Geographical and genetic diversity of the human hepatitis B virus. Hepatol Res;40:14-30.
9. Kao JH. Hepatitis B viral genotypes: clinical relevance and molecular characteristics. J Gastroenterol Hepatol 2002;17:643-650.
10. Orito E, Ichida T, Sakugawa H, Sata M, Horiike N, Hino K, et al. Geographic distribution of hepatitis B virus (HBV) genotype in patients with chronic HBV infection in Japan. HEPATOLOGY 2001;34: 590-594.
11. Matsuura K, Tanaka Y, Hige S, Yamada G, Murawaki Y, Komatsu M, et al. Distribution of hepatitis B virus genotypes among patients with chronic infection in Japan shifting toward an increase of genotype A. J Clin Microbiol 2009;47:1476-1483.
12. Ozasa A, Tanaka Y, Orito E, Sugiyama M, Kang JH, Hige S, et al. Influence of genotypes and precore mutations on fulminant or chronic outcome of acute hepatitis B virus infection. HEPATOLOGY 2006;44:326-334.
13. Kobayashi M, Ikeda K, Arase Y, Suzuki F, Akuta N, Hosaka T, et al. Change of hepatitis B virus genotypes in acute and chronic infections in Japan. J Med Virol 2008;80:1880-1884.
14. Mayerat C, Mantegani A, Frei PC. Does hepatitis B virus (HBV) genotype influence the clinical outcome of HBV infection? J Viral Hepat 1999;6:299-304.
15. Ogawa M, Hasegawa K, Naritomi T, Torii N, Hayashi N. Clinical features and viral sequences of various genotypes of hepatitis B virus compared among patients with acute hepatitis B. Hepatol Res 2002;23: 167-177.
16. Gilson RJ, Hawkins AE, Beecham MR, Ross E, Waite J, Briggs M, et al. Interactions between HIV and hepatitis B virus in homosexual men: effects on the natural history of infection. AIDS 1997;11:597-606.
17. Usuda S, Okamoto H, Iwanari H, Baba K, Tsuda F, Miyakawa Y, et al. Serological detection of hepatitis B virus genotypes by ELISA with monoclonal antibodies to type-specific epitopes in the preS2-region product. J Virol Methods 1999;80:97-112.
18. Usuda S, Okamoto H, Tanaka T, Kidd-Ljunggren K, Holland PV, Miyakawa Y, et al. Differentiation of hepatitis B virus genotypes D and E by ELISA using monoclonal antibodies to epitopes on the preS2-region product. J Virol Methods 2000;87:81-89.
19. Noto H, Terao T, Ryou S, Hirose Y, Yoshida T, Ookubo H, et al. Combined passive and active immunoprophylaxis for preventing perinatal transmission of the hepatitis B virus carrier state in Shizuoka, Japan during 1980-1994. J Gastroenterol Hepatol 2003;18:943-949.
20. Yoshikawa A, Suzuki K, Abe A, Tanaka T, Yamaguchi K, Ishikawa Y, et al. Effect of selective vaccination on a decrease in the rate of hepatitis B virus-positive Japanese first-time blood donors. Transfus Med 2009;19:172-179.
21. Lok AS, McMahon BJ. Chronic hepatitis B. HEPATOLOGY 2007;45:507-539.
22. Sato S, Ohhashi W, Ihara H, Sakaya S, Kato T, Ikeda H. Comparison of the sensitivity of NAT using pooled donor samples for HBV and that of a serologic HBsAg assay. Transfusion 2001;41:1107-1113.
23. Sherlock SDJ, editor. Virus hepatitis. London: Blackwell Scientific; 1997.
24. Tassopoulos NC, Papaevangelou GJ, Sjogren MH, Roumeliotou-Karayannis A, Gerin JL, Purcell RH. Natural history of acute hepatitis B surface antigen-positive hepatitis in Greek adults. Gastroenterology 1987;92:1844-1850.

25. McMahon BJ, Alward WL, Hall DB, Heyward WL, Bender TR, Francis DP, et al. Acute hepatitis B virus infection: relation of age to the clinical expression of disease and subsequent development of the carrier state. J Infect Dis 1985;151:599-603.
26. Kao JH, Chen DS. Global control of hepatitis B virus infection. Lancet Infect Dis 2002;2:395-403.
27. Chu CJ, Keeffe EB, Han SH, Perrillo RP, Min AD, Soldevila-Pico C, et al. Hepatitis B virus genotypes in the United States: results of a nationwide study. Gastroenterology 2003;125:444-451.
28. Livingston SE, Simonetti JP, Bulkow LR, Homan CE, Snoweball MM, Cagle HH, et al. Clearance of hepatitis B e antigen in patients with chronic hepatitis B and genotypes A, B, C, D, and F. Gastroenterology. 2007;133:1452-7.
29. Colin JF, Cazals-Hatem D, Loriot MA, Martinot-Peignoux M, Pham BN, Auperin A, et al. Influence of human immunodeficiency virus infection on chronic hepatitis B in homosexual men. HEPATOLOGY 1999;29:1306-1310.
30. Bocharov G, Ludewig B, Bertoletti A, Klenerman P, Junt T, Krebs P, et al. Underwhelming the immune response: effect of slow virus growth on CD8+-T-lymphocyte responses. J Virol 2004;78:2247-2254.
31. Sugiyama M, Tanaka Y, Kato T, Orito E, Ito K, Acharya SK, et al. Influence of hepatitis B virus genotypes on the intra- and extracellular expression of viral DNA and antigens. HEPATOLOGY 2006;44:915-924.
32. Ito K, Kim KH, Lok AS, Tong S. Characterization of genotype-specific carboxyl-terminal cleavage sites of hepatitis B virus e antigen precursor and identification of furin as the candidate enzyme. J Virol 2009;83: 3507-3517.
33. Milich D, Liang TJ. Exploring the biological basis of hepatitis B e antigen in hepatitis B virus infection. HEPATOLOGY 2003;38:1075-1086.
34. Lisotti A, Azzaroli F, Buonfiglioli F, Montagnani M, Alessandrelli F, Mazzella G. Lamivudine treatment for severe acute HBV hepatitis. Int J Med Sci 2008;5:309-312.
35. Jochum C, Gieseler RK, Gawlista I, Fiedler A, Manka P, Saner FH, et al. Hepatitis B-associated acute liver failure: immediate treatment with entecavir inhibits hepatitis B virus replication and potentially its sequelae. Digestion 2009;80:235-240.
36. Yu JW, Sun LJ, Zhao YH, Kang P, Li SC. The study of efficacy of lamivudine in patients with severe acute hepatitis B. Dig Dis Sci 2010;55: 775-783.
37. Kumar M, Satapathy S, Monga R, Das K, Hissar S, Pande C, et al. A randomized controlled trial of lamivudine to treat acute hepatitis B. HEPATOLOGY 2007;45:97-101.

Abdominal Imaging

Abdom Imaging (2015)
DOI: 10.1007/s00261-015-0352-9

Intratumoral artery on contrast-enhanced computed tomography imaging: differentiating intrahepatic cholangiocarcinoma from poorly differentiated hepatocellular carcinoma

Seiji Tsunematsu,[1] Makoto Chuma,[1,5] Toshiya Kamiyama,[2] Noriyuki Miyamoto,[3] Satoshi Yabusaki,[3] Kanako Hatanaka,[4] Tomoko Mitsuhashi,[4] Hirofumi Kamachi,[2] Hideki Yokoo,[2] Tatsuhiko Kakisaka,[2] Yousuke Tsuruga,[2] Tatsuya Orimo,[2] Kenji Wakayama,[2] Jun Ito,[1] Fumiyuki Sato,[1] Katsumi Terashita,[1] Masato Nakai,[1] Yoko Tsukuda,[1] Takuya Sho,[1] Goki Suda,[1] Kenichi Morikawa,[1] Mitsuteru Natsuizaka,[1] Mitsuru Nakanishi,[1] Koji Ogawa,[1] Akinobu Taketomi,[2] Yoshihiro Matsuno,[4] Naoya Sakamoto[1]

[1]Department of Gastroenterology and Hepatology, Graduate School of Medicine, Hokkaido University, 15 Kita, 7 Nishi, Kita-ku, Sapporo 060-8638, Japan
[2]Department of Gastroenterological Surgery, Graduate School of Medicine, Hokkaido University, Sapporo, Japan
[3]Department of Diagnostic and Interventional Radiology, Graduate School of Medicine, Hokkaido University, Sapporo, Japan
[4]Department of Surgical Pathology, Hokkaido University Hospital, Sapporo, Japan
[5]Gastroenterological Center, Yokohama City University Medical Center, Yokohama, Kanagawa, Japan

Abstract

Aim: Differentiating intrahepatic cholangiocarcinoma (ICC) from poorly differentiated hepatocellular carcinoma (p-HCC) is often difficult, but it is important for providing appropriate treatments. The purpose of this study was to examine the features differentiating ICC from p-HCC on contrast-enhanced dynamic-computed tomography (CT).
Methods: This study examined 42 patients with pathologically confirmed ICC (n = 19) or p-HCC (n = 23) for which contrast-enhanced dynamic CT data were available. CT images were analyzed for enhancement patterns during the arterial phase, washout pattern, delayed enhancement, satellite nodules, capsular retraction, lesion shape, and presence of an intratumoral hepatic artery, intratumoral hepatic vein, intratumoral portal vein, and bile duct dilation around the tumor, portal vein tumor thrombus, lobar atrophy, or lymphadenopathy.
Results: Univariate analysis revealed the presence of rim enhancement (p = 0.037), lobulated shape (p = 0.004), intratumoral artery ($p < 0.001$), and bile duct dilation (p = 0.006) as parameters significantly favoring ICC, while a washout pattern significantly favored p-HCC ($p < 0.001$). Multivariate analysis revealed intratumoral artery as a significant, independent variable predictive of ICC (p = 0.037), and 15 ICCs (78.9%) showed this feature. Washout pattern was a significant, independent variable favoring p-HCC (p = 0.049), with 15 p-HCCs (65.2%) showing this feature.
Conclusion: The presence of an intratumoral artery in the arterial phase on contrast-enhanced dynamic CT was a predictable finding for ICC, and the presence of a washout pattern was a predictable finding for p-HCC, differentiating between ICC and p-HCC.

Key words: Intrahepatic cholangiocarcinoma—Intratumoral artery—Poorly differentiated hepatocellular carcinoma—Contrast-enhanced CT—Differential diagnosis

Correspondence to: Makoto Chuma; *email:* chuma@yokohama-cu.ac.jp

Published online: 13 January 2015

Intrahepatic cholangiocarcinoma (ICC) is the second most common primary liver malignancy after hepatocellular carcinoma (HCC) and originates from the epithelial lining of the intrahepatic bile duct [1]. Several studies have shown that the incidences of ICC and HCC have been increasing [2–4]. Contrast-enhanced dynamic-computed tomography (CT) has a primary role to play in the differential diagnosis of focal liver lesions, including HCC and ICC. Bile duct dilatation and rim-like contrast enhancement are frequently seen on contrast-enhanced CT of ICC [5]. Classic advanced HCC appears as a round tumor showing intense hyperenhancement in the arterial phase, followed by washout during dynamic imaging [6]. Knowledge of the typical imaging features of ICC and HCC would facilitate accurate diagnosis in most cases.

However, advanced HCCs such as poorly differentiated HCC (p-HCC) might not be as hypervascular as classic HCC, which might cause difficulty in differentiation from ICC. Differentiating ICC from p-HCC can reduce the risk of inappropriate treatments for ICC, such as transarterial chemoembolization aimed at HCC. ICC is usually fatal because of the lack of effective non-surgical therapeutic modalities, so correct diagnosis of ICC based on radiological findings may have prognostic significance, particularly in determining treatment methods [7]. Furthermore, definitive diagnosis of ICC will help oncologists to consider adequate treatments, such as complete resection including lymph node dissection.

Although some reports have described the radiological characteristics of ICC and HCC [5, 6, 8, 9], no reports appear to have described imaging findings for pathologically confirmed ICC and p-HCC. On contrast-enhanced CT, intratumoral arteries were often seen in ICC. However, there have been no previous reports that intratumoral arteries on CT distinguish ICC from HCC.

The purpose of this study was to assess the CT features and enhancement patterns differentiating ICC from p-HCC; furthermore, we evaluated whether the presence of an intratumoral artery could be an independent predictor for differentiating ICC from p-HCC.

Methods

Patients

This study was approved by the ethics committees of Hokkaido University Hospital. All study protocols were approved by the institutional review board and performed in compliance with the Declaration of Helsinki.

We retrospectively searched the surgical treatment database at our hospital from July 2003 to December 2012, using the search terms "poorly differentiated HCC" and "ICC." Forty-two patients with histopathological confirmation of either ICC (n = 19) or p-HCC (n = 23) who had undergone contrast-enhanced CT in our institution were included in this study. The final diagnosis of all tumors was confirmed by histopathological examination of surgical specimens. Histological diagnosis was made according to World Health Organization criteria [10, 11]. Combined-type liver cancers were excluded to more clearly investigate differential points of CT imaging between poorly differentiated HCC and ICC. Patient demographics and tumor characteristics are summarized in Table 1.

The 19 patients with ICC included 13 men and 6 women (age range 48–79 years), while the 23 patients with p-HCC included 19 men and 4 women (age range 37–79 years). Serum levels of hepatitis B surface antigen and hepatitis C antibody, alpha-fetoprotein (AFP), protein induced by vitamin K absence or antagonist-II (PIVKA-II), carcinoembryonic antigen (CEA), and carbohydrate antigen 19-9 (CA19-9) were examined preoperatively in all patients.

Image analysis

CT images were obtained by using Aquilion 64 (n = 16, Toshiba Medical Systems, Tochigi, Japan), Aquilion 4-slice CT (n = 12, Toshiba Medical Systems, Tochigi, Japan), light Speed VCT (n = 6, GE, Waukesha, WI, USA), Somatom Volume Zoom (n = 4, Siemens Medical Solutions, Erlangen, Germany), and Somatom Sensation 64 (n = 4, Siemens AG Medical Solutions, Erlangen, Germany).

Unenhanced and 3-phase contrast-enhanced helical CT images were obtained. An automatic bolus-tracking program (Real Prep; Toshiba Medical Systems) was used to time the start of scanning for each phase after contrast material injection. Monitoring was performed at the level of the L1 vertebral body, with the region of interest cursor (0.8–2.0 cm^2) placed in the abdominal aorta. Real-time serial monitoring studies began 10 s after the start of contrast injection. The trigger threshold level was set at 200 Hounsfield units. Arterial phase and portal venous phase scanning started at 20 and 40 s after triggering, respectively. Delayed phase scanning started 180 s after the contrast injection. Contrast material (mean, 450 mg of iodine per kilogram body weight) was delivered over a period of 30 s.

Two radiologists (N.M. and S.Y. with 18 and 8 years of post-training experience in interpreting body CT images, respectively) who had no knowledge of clinical patient information performed all measurements by using a commercially available Digital Imaging and Communications in Medical viewer (VOX BASE; J-MAC, Sapporo, Japan).

The following CT features were evaluated: (1) lesion size; (2) satellite nodules (Fig. 1A); (3) capsular retraction (Fig. 1B); (4) lobulated shape of lesion (Fig. 1C); (5) rim enhancement during arterial phases (Fig. 1C); (6) intrahepatic bile duct dilation around the tumor

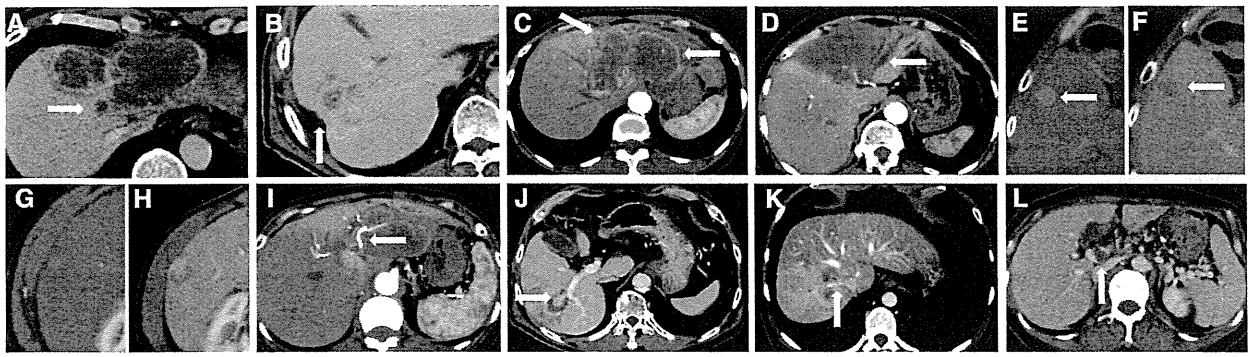

Fig. 1. Evaluated imaging features of contrast-enhanced CT for tumors. **A** CT during the arterial phase with p-HCC shows the satellite nodule (*arrows*). **B** CT during the delayed phase with ICC shows capsular retraction (*arrow*). **C, D** CT during the arterial phase with ICC shows a lobulated lesion and rim enhancement (*arrows*) (**C**) and intrahepatic bile duct dilation around the tumor (*arrow*) (**D**). **E, F** CT during the arterial phase (**E**) and delayed phase (**F**) with p-HCC shows arterial enhancement (**E**) and a washout pattern. **G, H** CT during the arterial phase (**G**) and delayed phase (**H**) with p-HCC shows delayed enhancement. **I–K** CT with ICC shows a hepatic artery running into the tumor (*arrow*) (**I**, arterial phase), a branch of the portal vein running into the tumor (*arrow*) (**J**, portal venous phase), and a hepatic vein running into the tumor (*arrow*) (**K**, delayed phase). **L** CT during the portal venous phase with p-HCC shows tumor thrombus in the portal vein (*arrow*).

Table 1. Patient characteristics of intrahepatic cholangiocarcinoma or poorly differentiated hepatocellular carcinoma

	ICC (n = 19)	p-HCC (n = 23)	p value
Gender (male/female)	13/6	19/4	0.283
Age (years)	63 (48–79)	62 (37–79)	0.535
Chronic viral hepatitis (HBV/HCV)	3 (2/1)	20 (11/9)	<0.001
Albumin (g/dL)	4.0 (3.1–4.6)	4.0 (3.1–5.2)	0.836
Total bilirubin (mg/dL)	0.8 (0.4–1.4)	0.9 (0.4–2.3)	0.389
Prothrombin time (%)	97 (79.3–135)	87 (66.1–111)	0.038
Platelet ($\times 10^4/\mu L$)	233 (122–354)	135 (42.0–305)	<0.001
AFP (10 ng/mL)	5.8 (2.3–80)	1360 (4.30–39,500)	<0.001
PIVKA-II (40 mAU/mL)	24 (7.0–1400)	208 (9.0–245,600)	0.002
CEA (5 ng/mL)	4.8 (1.0–345)	3.1 (1.4–9.1)	0.287
CA19-9 (37 U/mL)	45.1 (1.0–2590)	47.4 (1.0–237)	0.751

HBV hepatitis B virus, *HCV* hepatitis C virus, *AFP* alpha-fetoprotein, *PIVKA-II* protein induced by vitamin K absence or antagonist-II, *CEA* carcinoembryonic antigen, *CA19-9* cancer-associated carbohydrate antigen 19-9

(Fig. 1D); (7) arterial enhancement (Fig. 1E); (8) washout pattern (Fig. 1E, F); (9) delayed enhancement (Fig. 1G, H); (10) intratumoral artery during arterial phases (Fig. 1I); (11) intratumoral portal vein (Fig. 1J); (12) intratumoral hepatic vein (Fig. 1k) and portal vein tumor thrombus (Fig. 1L); (13) lobar atrophy; and (14) lymphadenopathy. The washout pattern was defined as arterial enhancement (due to the presence of non-triadal neo-angiogenetic arteries) and portal/venous wash out (due to the loss of sinusoidal vascularization) on dynamic imaging.

Particularly, an intratumoral artery was defined as an artery entering the tumor and remaining inside the tumor. Intratumoral portal veins and intratumoral hepatic veins were defined in a similar way. Although minimal discrepancies were seen between readers when interpreting the shape of lesions, consensus decisions for these discrepancies were easily reached during an additional reading session.

Statistical analysis

We statistically analyzed differences in clinical characteristics and CT imaging features between ICC and p-HCC by using the Chi square test for categorical variables and the non-parametric Mann–Whitney U test for continuous variables. Significant variables obtained from univariate analysis were applied to multivariate stepwise binary logistic regression analysis to determine the optimal findings for differentiating ICC from p-HCC. Statistical analyses were performed by using the SPSS software package, version 20.0 (IBM, NY). For all tests, values of $p < 0.05$ were considered statistically significant.

Results

Characteristics of patients with ICC or p-HCC

Baseline characteristics of patients with ICC or p-HCC are summarized in Table 1. There were no significant

Table 2. Uni- and multivariate analysis of contrast-enhanced CT features of intrahepatic cholangiocarcinoma and poorly differentiated hepatocellular carcinoma

Pattern	ICC (n = 19)	p-HCC (n = 23)	Univariate analysis p	Multivariate analysis	
				p	Odds ratio (95% CI)
Mean diameter (mm)	64.4 (25–150)	53.7 (10–150)	0.192		
Lobulated shape	14 (73.7)	9 (39.1)	0.004	0.550	1.951 (0.218–17.445)
Satellite nodule	15 (78.9)	14 (60.1)	0.207		
Capsular retraction	6 (31.6)	5 (21.7)	0.407		
Arterial enhancement	9 (47.3)	17 (73.9)	0.078		
Bile duct dilatation	11 (57.9)	4 (17.4)	0.006	0.323	3.445 (0.296–40.070)
Rim enhancement	13 (48.4)	4 (17.4)	0.037	0.158	6.068 (0.495–74.308)
Delayed enhancement	8 (42.1)	7 (30.4)	0.432		
Washout	1 (5.3)	15 (65.2)	<0.001	0.049	0.087 (0.008–0.993)
Intratumoral artery	15 (78.9)	8 (34.8)	<0.001	0.037	10.192 (1.155–89.954)
Intratumoral portal vein	7 (36.8)	2 (8.7)	0.055		
Intratumoral vein	3 (15.8)	2 (8.7)	0.581		
Portal vein tumor thrombus	1 (5.3)	4 (17.4)	0.197		
Lobar atrophy	6 (31.6)	2 (8.7)	0.060		
Lymphadenopathy	4 (21.1)	1 (4.3)	0.094		

Values in parentheses represent percentages

differences between the 2 groups with regard to sex, age, albumin, total bilirubin, CEA, and CA19-9. However, there were differences with respect to chronic viral hepatitis, prothrombin time, platelet counts, AFP, and PIVKA-II.

Analyses of contrast-enhanced CT features of ICC and p-HCC

CT features of ICC and p-HCC and the results of univariate analysis are summarized in Table 2. Lesion diameter ranged from 2.5 to 15.0 cm (mean 64.4 mm) for ICC and from 1.0 to 15.0 cm (mean 53.7 mm) for p-HCC (p = 0.192). Lobulated lesion shape was significantly more rare in patients with p-HCC (n = 9, 39.1%) than in patients with ICC (n = 14, 73.7%) (p = 0.004). The presence of satellite nodules was not statistically significantly different between ICC (n = 15, 78.9%) and p-HCC (n = 14, 60.1%) (p = 0.207). Significant differences in arterial enhancement were not seen between ICC (n = 9, 47.3%) and p-HCC (n = 17, 73.9) (p = 0.078). Capsular retraction was present in patients with ICC (n = 6, 31.6%) or p-HCC (n = 5, 21.7%) (p = 0.407). The presence of intrahepatic bile duct dilation around the tumor differed significantly between the ICC group (n = 11, 57.9%) and the p-HCC group (n = 4, 17.4%) (p = 0.006). Peripheral rim enhancement in the arterial phase was less common in the p-HCC group (n = 4, 17.4%) than in the ICC group (n = 13, 48.4%) (p = 0.037). A washout pattern was more frequent in p-HCC (n = 15, 65.2%) than ICC (n = 1, 5.3%) (p < 0.001). There was no significant difference (p = 0.432) in the occurrence of delayed enhancement in p-HCC (n = 8, 42.1%) and in ICC (n = 7, 30.4%).

An intratumoral artery in the arterial phase was more frequently present for ICC lesions (n = 15, 78.9%) than p-HCC (n = 8, 34.8%) (p < 0.001). The ICC group more frequently showed an intratumoral portal vein (n = 7, 36.8%) than the p-HCC group (n = 2, 8.7%) (p = 0.055). An intratumoral hepatic vein was rarely exhibited in ICCs (n = 3, 15.8%) or p-HCCs (n = 2, 8.7%) (p = 0.581). Portal vein tumor thrombus was also rarely present in ICCs (n = 1, 5.3%) or p-HCCs (n = 4, 17.4%) (p = 0.197).

There was no significant difference (p = 0.060) in the presence of lobar atrophy in ICC (n = 6, 31.6%) and in p-HCC (n = 2, 8.7%). Lymphadenopathy was present in patients with ICC (n = 4, 21.1%) or p-HCC (n = 1, 4.3%) (p = 0.407).

Next, we conducted multivariate binary logistic regression analysis by using significant parameters from the univariate analysis. As shown in Table 2, the presence of an intratumoral artery was an independent CT predictor for differentiating ICC from p-HCC (p = 0.037, odds ratio = 10.192); on the contrary, washout pattern was a significant parameter favoring p-HCC (p = 0.049, odds ratio = 0.087). The presence of an intratumoral artery on CT had a sensitivity of 78.9% and a specificity of 65.2% for ICC. Furthermore, the presence of an intratumoral artery on CT had a positive predictive value of 65.2% and a negative predictive value of 78.9% for ICC.

Case presentation

Representative images from CT and histological features in patients with ICC and p-HCC are shown in Figs. 2 and 3. A 60-year-old man (Case 1) presented with a massive, advanced tumor predominantly located in the right lobe of the liver, and a hepatic artery was seen running into the tumor on CT (Fig. 2A). A right hepatic lobectomy was performed, and histological examination revealed ICC tumor cells that showed infiltrating

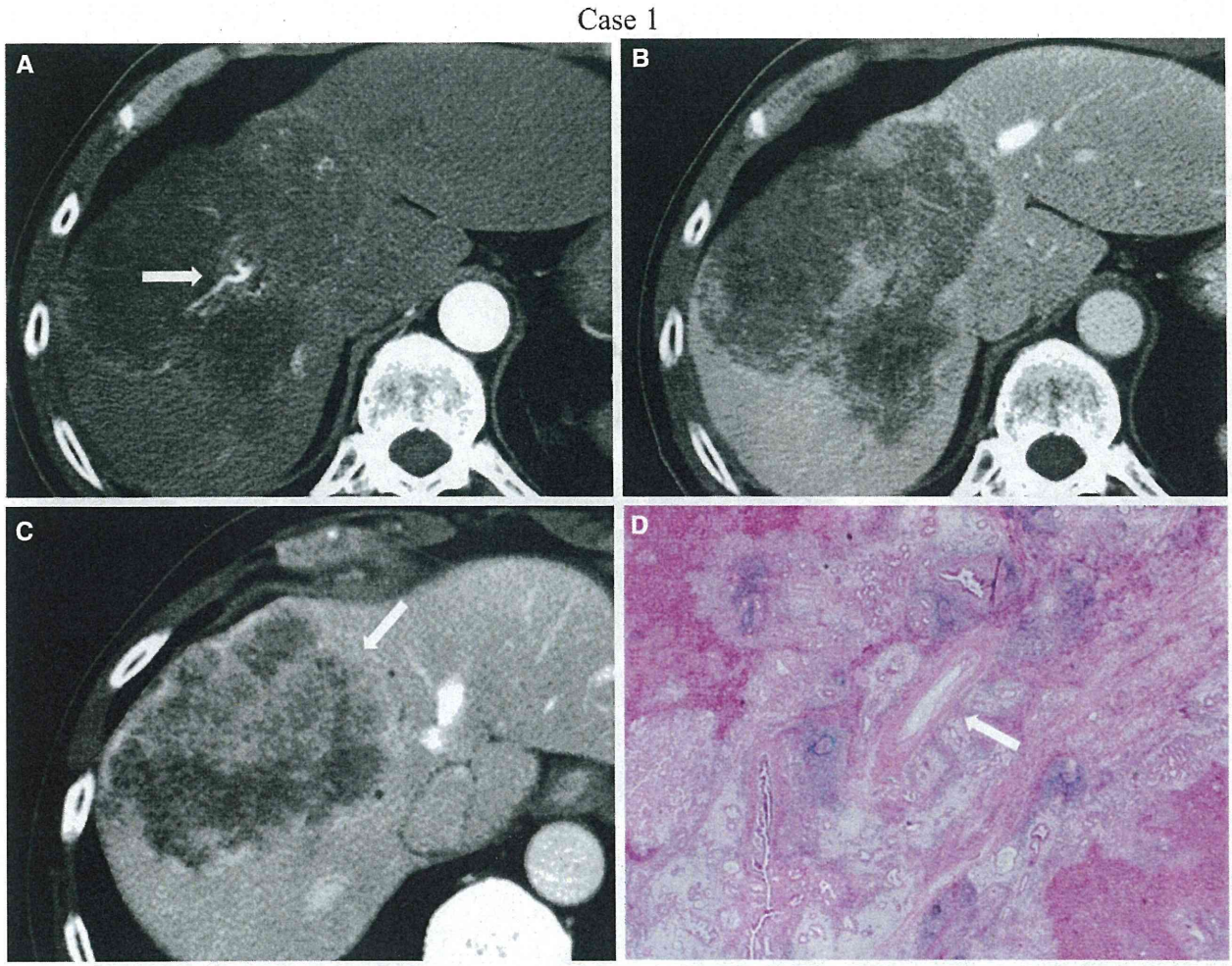

Fig. 2. Contrast-enhanced CT and histological features of ICC. **A** ICC in a 60-year-old man shows a subtle intratumoral artery on arterial phase CT (*arrow*). **B**, **C** CT on delayed phase shows the absence of delayed enhancement (**B**) and the presence of a lobulated shape (**C**). **D** ICC tumor cells show infiltrating replacement growth of the surrounding hepatic parenchyma. An intratumoral artery that has not been destroyed by tumor cells is identified (*arrow*). (Original magnification: d × 10. Hematoxylin and eosin staining).

replacement growth against the surrounding hepatic parenchyma. An intratumoral artery that had not been destroyed by tumor cells was identified (Fig. 2D). A 58-year-old woman (Case 2) presented with a massive, advanced tumor predominantly located in the left lobe of the liver, and no intratumoral artery, portal vein, or hepatic vein was identified on CT (Fig. 3A). A left hepatic lobectomy was performed, and histological examination revealed p-HCC. The tumor was compressing the surrounding liver, and compressed vessels were clearly visible (Fig. 3D).

Discussion

On contrast-enhanced CT, the typical appearance of ICC is a mass that demonstrates thin, rim-like, or thick, band-like contrast enhancement around the tumor during arterial and portal venous phases, with satellite nodules, capsular retraction, lobar atrophy, lymphadenopathy, and delayed enhancement [12–15]. The accuracy of contrast-enhanced CT in diagnosing ICC was 70% [16]. The finding of satellite nodules was associated with tendency to invade small portal vessels and along portal triads. Additionally, scirrhous stroma and biliary involvement of ICC have an influence on the imaging of capsular retraction and lobar atrophy. In our study, a lobulated shape was more closely associated with ICC than with p-HCC on univariate analysis, although satellite nodules, capsular retraction, lobar atrophy, and lymphadenopathy were not different between ICC and p-ICC. The finding of lobulated shape supported the results of previous studies [17, 18]. This trend may be

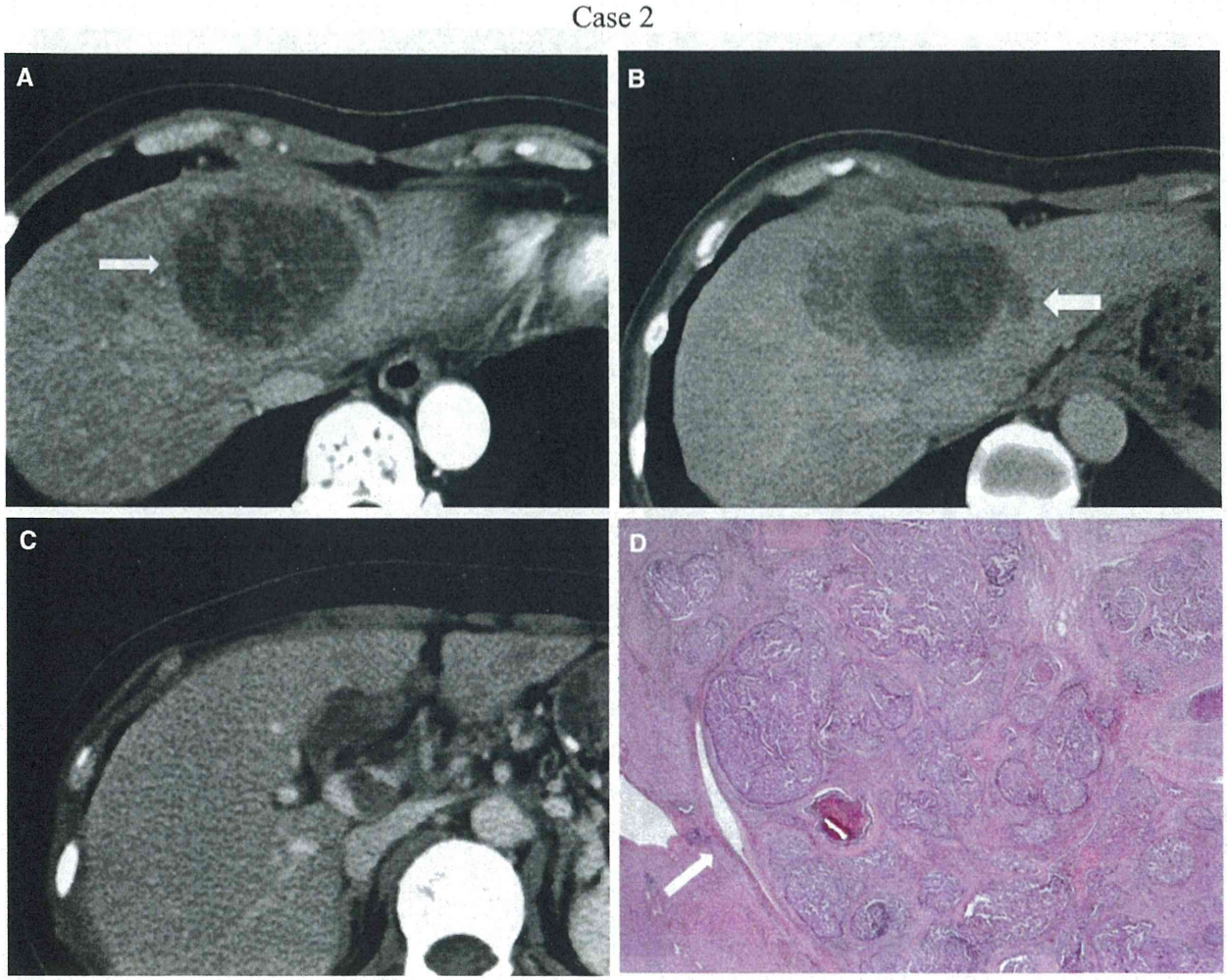

Fig. 3. Contrast-enhanced CT and histological features of p-HCC. **A** p-HCC in a 58-year-old woman shows a low attenuating tumor on arterial phase CT (*arrow*). **B** CT on delayed phase shows nodule (*arrow*) and the absence of delayed enhancement. **C** CT on portal venous phase shows portal vein tumor thrombus. **D** Compressive growth of p-HCC. Tumor compresses the surrounding liver and compressed vessels are clearly visible (*arrow*). (Original magnification: d × 10. Hematoxylin and eosin staining).

related to the fact that ICC tends to invade small portal vein branches adjacent to the main tumor, and the fusion of the primary mass and adjacent satellite tumors results in the lobulated shape [19]. Tumor shape could thus represent a differential feature between ICC and p-HCC.

The frequency of intrahepatic bile duct dilation around the tumor differed between ICC and p-HCC. Eleven of the 19 ICC tumors were accompanied by intrahepatic bile duct dilation around the tumor. The presence of intrahepatic bile duct dilation around the tumor may thus provide a useful clue for differentiation.

In our study, 13 ICC showed rim enhancement during the arterial phase. Rim enhancement patterns differing from p-HCC may relate to different pathological components in the tumor [20]. Fan et al. suggested that the degree of enhancement of ICC depends on the proportion of component fibers and tumor cells, with a tumor rich in cells resulting in strong enhancement [9]. ICC that is peripherally rich in tumor cells with fibrosis in the central portion may result in peripheral rim-like hyperenhancement.

In addition, significant differences in washout patterns were seen between ICC and p-HCC, although there were no significant differences in arterial enhancement and delayed enhancement between the two groups. According to the guidelines of the American Association for the Study of Liver Disease, nodules larger than 1 cm detected in liver cirrhosis may be confidently diagnosed as HCC only when a washout pattern is detected on contrast-enhanced CT or magnetic resonance imaging

[21]. According to our findings, the washout pattern can be useful for identifying p-HCC or ICC. However, distinguishing p-HCC from some ICCs showing diffuse hyperenhancement in the arterial phase and subsequent washout is difficult.

In our present study, 15 (78.9%) of the 19 ICCs showed an intratumoral artery in the arterial phase. Although we occasionally recognized vessels running into the tumor, to the best of our knowledge, no previous reports have described the presence of intratumoral arteries in ICC and p-HCC. In our study, ICCs were able to be differentiated from p-HCCs based on the finding of an intratumoral artery ($p = 0.037$), according to multivariate binary logistic regression analysis. Based on our results, the presence of an intratumoral artery in the arterial phase on contrast-enhanced CT could be a predictive finding for reliable differentiation of ICC from p-HCC. Few reports have described intratumoral arteries of ICC being demonstrated on contrast-enhanced CT. One study showed intratumoral arteries of the ICC identified immediately after the injection of contrast material for CT during hepatic arteriography [22]. Furthermore, that study indicated that tumor enhancement gradually spreads from each intratumoral artery [22]. Infiltrating replacement is an inherent growth feature of ICC, with the surrounding liver gradually incorporated into the tumor as it grows [23]. In this process, the blood vessel is not destroyed by tumor cells and is retained inside. By contrast, HCC shows fibrous encapsulation or compressive growth [24]. With such growth, blood vessels are pressed to the outside of the tumor. Our cases also showed these features (Fig. 2). Such differences in growth type may be related to differences in intratumoral arteries between ICC and HCC. No significant difference was seen between ICC and p-HCC in regard to intratumoral portal veins, intratumoral hepatic veins, or portal vein tumor thrombus. We supposed that intratumoral artery was retained within the ICC rather than portal or hepatic veins because of the stiffness of the arterial wall.

The results of this study have revealed features that allow ICC and p-HCC to be distinguished based on findings from contrast-enhanced CT. In clinical practice, contrast-enhanced CT is a useful diagnostic method to distinguish ICC from p-HCC, since results of tumor marker levels and tissue biopsy are difficult and often indeterminate. The optimal treatment for ICC is complete tumor resection, including lymph node removal [25–27]. In cases of HCC, the treatment modality of choice depending on the degree of cirrhosis is complete resection, topical therapy including radiofrequency ablation or liver transplantation. If the patient has advanced cirrhosis or advanced HCC, then treatments such as transarterial chemoembolization hepatic arterial infusion chemotherapy and systemic chemotherapy are applicable [28, 29]. Because misdiagnosis of ICC as HCC can lead to inadequate medical care, our identification of characteristic findings for ICC may have important practical value in attaining a correct diagnosis.

This study has several limitations that must be considered when interpreting the results. First, our study might have included some degree of selection bias, as we retrospectively analyzed only those patients with ICC or p-HCC who underwent contrast-enhanced CT and hepatic surgery. The absence of the well- and moderately differentiated subtypes of HCC in this study is an important limitation in interpreting our results. Additionally, the numbers of ICCs and p-HCCs were relatively small, because the patient group was limited to those with a pathologic diagnosis determined by surgery. Finally, most tumors were relatively large, and the findings in our results may not be observed in smaller sized tumors.

In conclusion, the presence of an intratumoral artery during arterial phase on enhanced CT is valuable in differentiating between ICC and p-HCC, as is the washout pattern. This new finding may facilitate correct diagnosis and more timely selection of appropriate treatment strategies.

Acknowledgments. This study was supported by Grants from the Ministry of Education, Culture, Sports, Science and Technology-Japan; Ministry of Health, Labour and Welfare-Japan; and Japan Health Sciences Foundation.

Conflict of interest. The authors declare that they have no conflicts of interest.

References

1. Kham SA, Thomas HC, Davidson BR, et al. (2005) Cholangiocarcinoma. Lancet 366:1303–1314
2. Patel T (2001) Increasing incidence and mortality of primary intrahepatic cholangiocarcinoma in the United States. Hepatology 33:1353–1357
3. Singh P, Patel T (2006) Advances in the diagnosis, evaluation and management of cholangiocarcinoma. Curr Opin Gastroenterol 22:294–299
4. Shaib Y, El-Serag HB (2004) The epidemiology of cholangiocarcinoma. Semin Liver Dis 24:115–125
5. Valls C, Guma A, Puig I, et al. (2000) Intrahepatic peripheral cholangiocarcinoma: CT evaluation. Abdom Imaging 25:490–496
6. Bruix J, Sherman M (2005) Practice Guidelines Committee, American Association for the Study of Liver Diseases. Management of hepatocellular carcinoma. Hepatology 42:1208–1236
7. Khan SA, Davidson BR, Goldin R, et al. (2002) Guidelines for the diagnosis and management of cholangiocarcinoma. Gut 61:1657–1669
8. Choi BI, Han JK, Shin YM, et al. (1995) Peripheral cholangiocarcinoma: comparison of MRI with CT. Abdom Imaging 20:357–360
9. Fan ZM, Yamashita Y, Harada M, et al. (1993) Intrahepatic cholangiocarcinoma: spin-echo and contrast-enhanced dynamic MR imaging. Am J Roentgenol 161:313–317
10. Hirohashi S, Ishak KG, Kojiro M, et al. (2000) Hepatocellular carcinoma. In: Hamilton SRAL (ed) *World Health Organization classification of tumours pathology and genetics of tumours of the digestive system.* Lyon: IARC Press, pp 159–172
11. Nakanuma Y, Leong AS-Y, Sripa B, et al. (2000) Intrahepatic cholangiocarcinoma. In: Hamilton SR (ed) *World Health Organization classification of tumours Pathology and genetics of tumours of the digestive system.* Aaltonen: IARC Press, pp 173–180

12. Lee WJ, Lim HK, Jang KM, et al. (2001) Radiologic spectrum of cholangiocarcinoma: emphasis on unusual manifestations and differential diagnosis. Radiographics 21:97–116
13. Han JK, Choi BI, Kim AY, et al. (2002) Cholangiocarcinoma: pictorial essay of CT and cholangiographic findings. Radiographics 22:173–187
14. Baheti AD, Tirumani SH, Rosenthal MH, Shinagare AB, Ramaiya NH (2014) Diagnosis and management of intrahepatic cholangiocarcinoma: a comprehensive update for the radiologist. Clin Radiol 69:e463–e470
15. Kim TK, Choi BI, Han JK, et al. (1997) Peripheral cholangiocarcinoma of the liver: two-phase helical CT findings. Radiology 204:539–543
16. Olnes MJ, Erlich R (2004) A review and update on cholangiocarcinoma. Oncology 66:167–179
17. Choi BI, Han JK, Shin YM, et al. (1995) Peripheral cholangiocarcinoma: comparison of MRI with CT. Abdom Imaging 20:357–360
18. Valls C, Guma A, Puig I, et al. (2000) Intrahepatic peripheral cholangiocarcinoma: CT evaluation. Abdom Imaging 25:490–496
19. Lim JH (2003) Cholangiocarcinoma: morphologic classification according to growth pattern and imaging findings. Am J Roentgenol 181:819–827
20. Ros PR, Buck JL, Goodman ZD, et al. (1988) Intrahepatic cholangiocarcinoma: radiologic-pathologic correlation. Radiology 167:689–693
21. Bruix J, Sherman M (2011) American association for the study of liver diseases. Management of hepatocellular carcinoma: an update. Hepatology 53:1020–1022
22. Miura F, Okazumi S, Takayama W, et al. (2004) Hemodynamics of intrahepatic cholangiocarcinoma: evaluation with single-level dynamic CT during hepatic arteriography. Abdom Imaging 29:467–471
23. Kozaka K, Sasaki M, Fujii T, et al. (2007) A subgroup of intrahepatic cholangiocarcinoma with an infiltrating replacement growth pattern and a resemblance to reactive proliferating bile ductules: bile ductular carcinoma. Histopathology 51:390–400
24. Ueda K, Terada T, Nakanuma Y, et al. (1992) Vascular supply in adenomatous hyperplasia of the liver and hepatocellular carcinoma: a morphometric study. Hum. Pathol 23:619–626
25. Singh P, Patel T (2006) Advances in the diagnosis, evaluation and management of cholangiocarcinoma. Curr Opin Gastroenterol 22:294–299
26. Jarnagin WR, Shoup M (2004) Surgical management of cholangiocarcinoma. Semin Liver Dis 24:189–199
27. Nagorney DM, Donohue JH, Farnell MB, et al. (1993) Outcomes after curative resections of cholangiocarcinoma. Arch Surg 128:871–879
28. Bruix J, Sherman M, Llovet JM, et al. (2001) Clinical management of hepatocellular carcinoma: conclusions of the Barcelona-2000 EASL conference. J Hepatol 35:421–430
29. Hertl M, Cosimi AB (2005) Liver transplantation for malignancy. Oncologist 10:269–281

Abdominal Imaging

Abdom Imaging (2014)
DOI: 10.1007/s00261-014-0296-5

Use of transabdominal ultrasonography to preoperatively determine T-stage of proven colon cancers

Susumu Shibasaki,[1] Norihiko Takahashi,[1] Shigenori Homma,[1] Mutsumi Nishida,[2] Tatsushi Shimokuni,[1] Tadashi Yoshida,[1] Hideki Kawamura,[1] Noriko Oyama-Manabe,[3] Kohsuke Kudo,[3] Akinobu Taketomi[1]

[1]Department of Gastroenterological Surgery I, Hokkaido University Graduate School of Medicine, N15, W7, Kita-Ku, Sapporo, Hokkaido 060-8638, Japan
[2]Division of Laboratory and Transfusion Medicine, Diagnostic Center for Sonography, Hokkaido University Hospital, Sapporo, Hokkaido, Japan
[3]Department of Diagnostic and Interventional Radiology, Hokkaido University Hospital, Sapporo, Hokkaido, Japan

Abstract

Purpose: Although noninvasive and highly informative, transabdominal ultrasonography (US) is not yet an accepted means of staging colorectal cancer preoperatively. This prospective study evaluated the diagnostic accuracy of US in preoperative staging of patients with resectable colon cancers. *Methods*: A total of 98 patients with primary colon cancer diagnosed by colonoscopy at our institute between January, 2011 and June, 2014 underwent preoperative ultrasonographic tumor staging. Depth of tumor infiltration (T-stage) was assessed by standard means (i.e., extent of mural involvement), analyzing agreement in US and histopathology determinations. *Results*: All but two colon cancers (at splenic flexure) were detected by US (98%, 96/98). Compared with histopathology, overall accuracy of US in determining T-stage was 64% (61/96), indicating moderate reproducibility (κ coefficient 0.48; 95% CI 0.35–0.62; $p < 0.001$). Using a three-tier approach of graded muscularis propria (MP) involvement (Tis/T1, below MP; T2, within MP; and T3/T4, beyond MP), diagnostic agreement increased to 89% (85/96), with good agreement (κ coefficient 0.77; 95% CI 0.64–0.90; $p < 0.001$). No tumor characteristics or patient demographics influenced diagnostic agreement at any site in the colon. *Conclusions*: Given the potential to yield valuable information while limiting patient discomfort, US should be reconsidered as a means of assessing colon cancer.

Correspondence to: Susumu Shibasaki; *email:* susumushi48@mist.ocn.ne.jp

Published online: 16 November 2014

Key words: Colon cancer—Transabdominal ultrasonography—Preoperative T-stage diagnosis

Accurate preoperative assessments are essential for devising appropriate surgical strategies and predicting the prognosis of patients with resectable colorectal cancers. Factors such as depth of intestinal mural tumor infiltration (T-stage) and adjacent organ invasion have bearing on various aspects of planned surgical procedures, including operative approach, extent of resection, and method of anastomosis. Similarly, preoperative determination of tumor spread beyond muscularis propria (MP) is an important prognosticator, associated with a poor outcome in patients with colorectal cancer [1]. By helping to gage the extent of needed lymph node (LN) dissection, reliable and precise assessment of T-stage also contributes to optimal surgical outcomes.

Transabdominal ultrasonography (US) is widely used to screen and investigate patients with abdominal tumors (e.g., hepatobiliary, pancreatic, and gynecologic), because it is cost-effective and noninvasive. Although US may be used to delineate abnormal intestinal features, such as thickening of bowel wall, loss of defined bowel wall layers, and lack of compressibility [2], its value in clinical staging of gastrointestinal tumors has been curtailed by problematic bowel gas and the relative thinness of normal intestinal wall. Hydrosonography, an US technique used to visualize the colon through retrograde water infusion, has yielded high rates of tumor detection (89.7%), as well as high accuracy (85.2%) of determining

T-stage preoperatively in patients with colorectal cancer [3]. However, hydrosonography is not in common use due to its complicated setup and the physical and psychological distress imposed on patients during examinations.

In recent years, US has grown better suited for detecting colorectal cancer through better quality equipment. Image resolution and attenuating effect of deeper echogenicity have both greatly improved [4–7]. However, related studies have often focused on sensitivity and specificity, and preoperative staging investigations have targeted patients with gastric cancer [8–11]. To our knowledge, there are no existing reports on the use of US to assess colorectal cancer. The aim of this study was to evaluate the merit of US in preoperative determinations of T-stage, enlisting a population of patients already diagnosed (via colonoscopy) with colon cancer, and to establish practical diagnostic criteria for US in this specific context.

Materials and methods

Patients

A total of 98 patients with primary colon cancer diagnosed at our institute via colonoscopy between January, 2011 and June, 2014 were included for study. All patients granted informed written consent, and this study was approved by our Institutional Review Board. In each instance, transabdominal US was performed to determine T-stage and was executed by ultrasound technicians who were aware of tumor sites (based on colonoscopy reports). Surgical treatment was undertaken at our institution within 1 month after such examinations.

Included in the study population were 60 males and 38 females, with median age of 68 years (range 30–86 years). Twenty of these patients had clinical stage IV tumors (sites of metastasis: liver, 14; lung, 4; peritoneum, 4; and distant lymph node, (1), and seven had multiple metastases. Each initial diagnosis of synchronous metastasis was confirmed by US, computed tomography (CT), and magnetic resonance imaging (MRI). MRI diagnostics were not intended for preoperative determinations of colon cancer T-stage. In addition, our sonographers were blinded to results of endoscopic US, which was performed in just three patients. All US findings were evaluated prospectively, whereas histopathology results were retrospectively reviewed.

Transabdominal ultrasonography

An Aplio^{TM} SSA-770A/790A ultrasound unit (Toshiba Medical Systems Corp., Otawara, Tochigi, Japan), with a 3.75/5.8 MHz center frequency convex transducer (PVT-375BT/674BT) or a 7.0 MHz center frequency linear transducer (PLT-705BTH) was used for each examination. An 8-h fast was stipulated prior to the procedure, which otherwise required no intake of water or added preparations. Patients generally remained supine during examinations or were moved to decubitus position as needed. Colon and rectum were sequentially assessed, first locating hepatic flexure; then scanning ascending colon toward cecum, identifying terminal ileum and Bauhin's valve; and finally tracing colon from cecum to sigmoid colon. All US procedures were carried out by eight sonographers, each a registered medical sonographer, certified by the Japan Society of Ultrasonics in Medicine (JSUM). All still images and movie clips were analyzed and interpreted by a registered senior sonographer with >25 years of experience in US—one of only eight such JSUM-certified experts in the country of Japan. All data interpretation was under the direction of radiologists.

Diagnostic criteria of T-stage in ultrasonographic evaluations

Normal intestinal wall, usually divisible into five distinct layers on sonograms [12], is shown in Fig. 1. Colorectal cancers typically appear as focal hypoechoic masses of irregular shape, showing segmental circumferential thickening of bowel wall. Abnormal colorectal wall

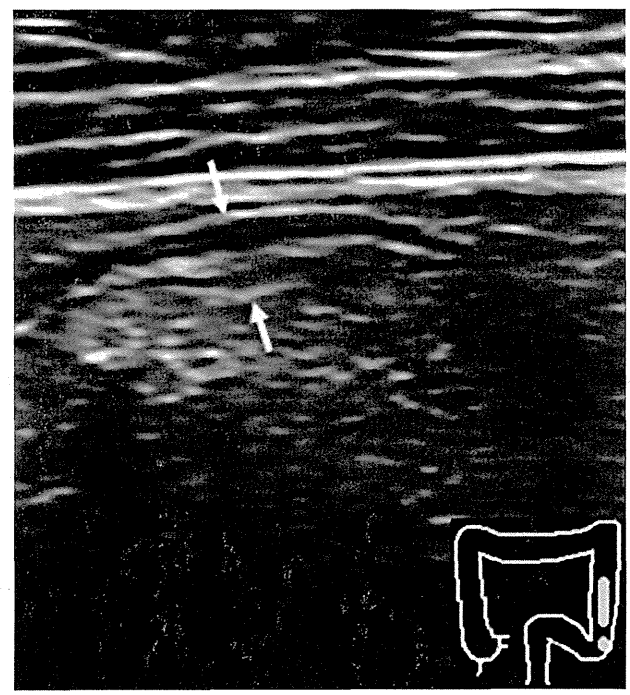

Fig. 1. Normal colonic wall on transabdominal US, depicted as five distinct layers (*white arrows*): (1) inner hyperechoic layer, or interface between mucosa and bowel contents; (2) hypoechoic layer, representing deep mucosa; (3) hyperechoic layer, which is submucosa; (4) hypoechoic layer, most easily recognized layer of muscularis propria (MP); and (5) outer hyperechoic layer, composed of serosa and serosal fat.

thickening was defined as a diameter >2 mm, as previously reported [7, 8]. Guidelines of the Japanese Society for Cancer of the Colon and Rectum (2010) [13] were applied to assign T-stage by US as follows: Tis, focal hypoechoic mass in contact with mucosa or deep mucosa; T1, focal hypoechoic mass infiltrating submucosa, without involving MP; T2, focal hypoechoic mass invading MP; T3, focal hypoechoic mass penetrating MP but not infiltrating adjacent organs; and T4, hypoechoic mass penetrating serosal surface. Representative US findings for the T-stage of each tumor are shown in Figs. 2, 3, 4, 5 and 6.

CT evaluation

Patients routinely underwent thoracic, abdominal, and pelvic contrast-enhanced CT scanning to evaluate nodal and distant metastases. CT examination entailed contrast-enhanced single-phase imaging, using a 5-mm slice thickness. CT images were interpreted by experienced radiologists. Due to difficulty visualizing the individual bowel wall layers, T-stage assessment by CT was usually limited to predicting whether tumor had penetrated the serosa or adjacent organs, rather than speculating on configuration of tumor margins, as previously reported [14]. Two patients with clinically suspected tumor invasion of other organs by CT were excluded from study.

Histopathologic evaluation

Samples from all formalin-fixed resections were embedded in paraffin, sectioned, and routinely stained (hematoxylin and eosin). Histopathologic evaluation was performed at our facility by pathologist specializing in colorectal cancer. T-stage was assigned according to

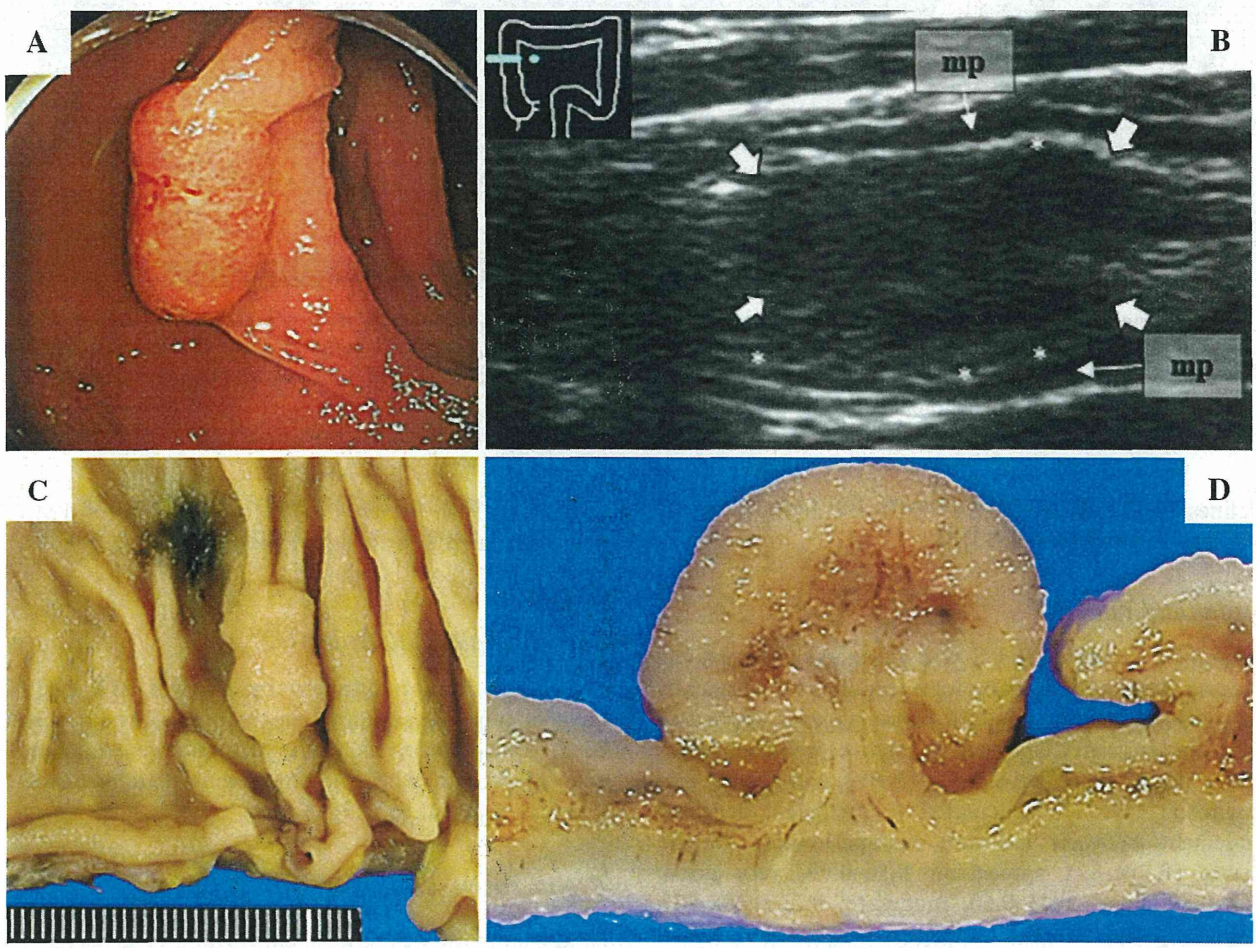

Fig. 2. Representative sonograph of stage Tis tumor. **A** Type 0-Isp tumor of ascending colon on colonoscopy. **B** Hypoechoic tumor as localized mural thickening (*larger white arrows*) on transabdominal US. Muscularis propria (*MP, smaller white arrows*) distinguishable as hypoechoic layer. Submucosa appears as hyperechoic layer (*) above MP. Stage Tis assigned based on continuity of submucosa. **C** and **D** Resected tumor shown, confirmed as stage Tis by histopathology.

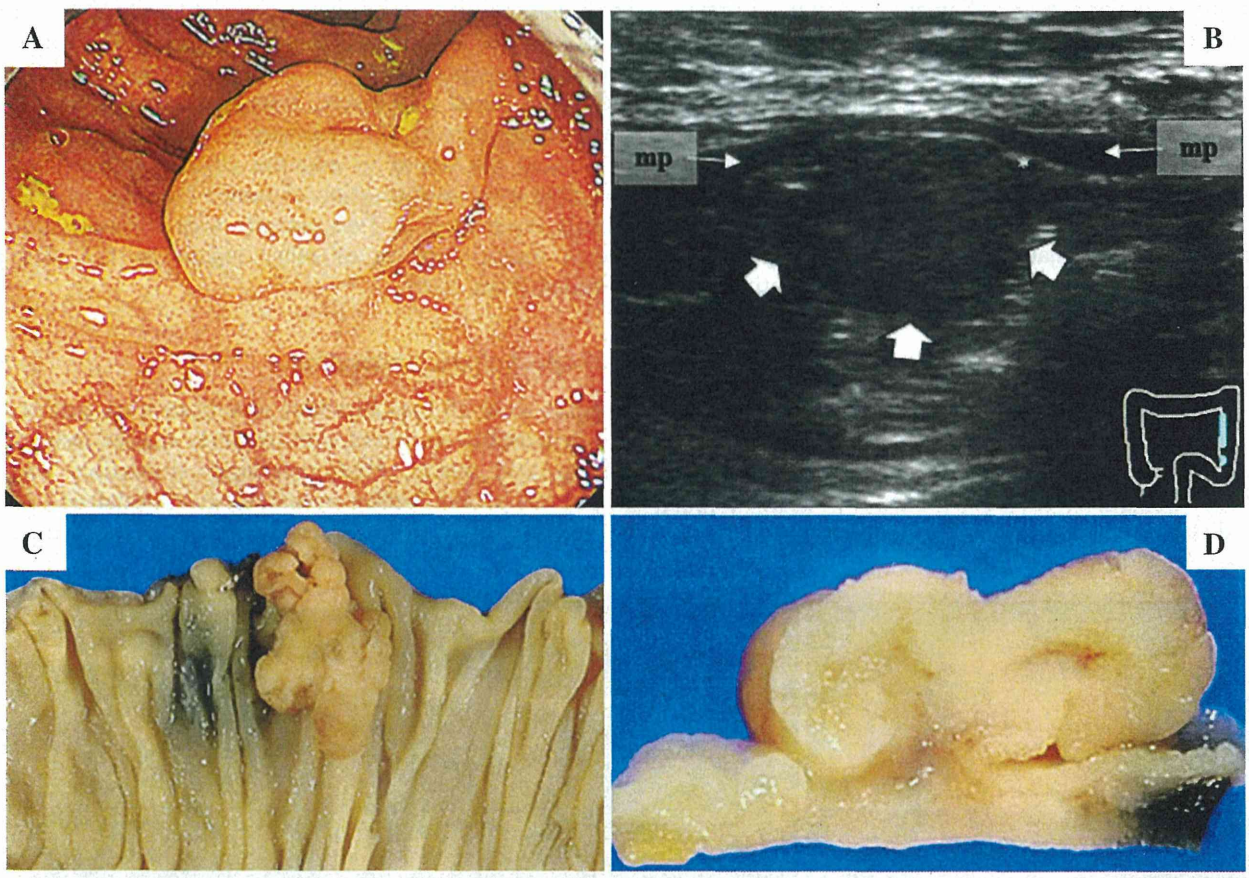

Fig. 3. Representative sonograph of stage T1 tumor. **A** Type 0-Isp tumor of descending colon on colonoscopy. **B** Hypoechoic tumor as mural thickening (*larger white arrows*) on transabdominal US. Muscularis propria (*MP, smaller white arrows*) distinguishable as hypoechoic layer. Submucosa appears as hyperechoic layer (*) above MP. Stage T1 assigned based on irregularity of submucosa and intact MP layer. **C** and **D** Resected tumor shown, confirmed as stage T1 by histopathology.

guidelines of the Japanese Society for Cancer of the Colon and Rectum (2010) [13].

Statistical analysis

Diagnostic accuracy of US was assessed by comparing imaging results with pathologic findings of surgically removed specimens. Standard formulas were applied to calculate sensitivity, specificity, positive predictive value (PPV), negative predictive value (NPV), and accuracy of diagnostic US. The calculated κ coefficient reflected agreement between US and histopathologic staging results (1, perfect agreement; 0.80–0.99, very good; 0.61–0.80, good; 0.41–0.60, moderate; 0.21–0.40, fair; and ≤0.20, poor). A 95% confidence interval (CI) was estimated from standard error. Spearman's rank correlation coefficient was also calculated to assess data correlation. Comparisons of qualitative variables relied on the Chi squared test (Yates' correction when necessary) for independence. Standard software was used for statistical analysis (StatMate IV for Windows; ATMS Co, Tokyo, Japan), with significance set at $p < 0.05$.

Results

Tumor identification by US

The rate of tumor detection by US was 98% (96/98). Each of two T1 tumors of descending colon (at splenic flexure) were under 15 mm in size and were unidentifiable. Median thickness of bowel wall at tumorous sites was 12.1 mm (range, 2.3–58 mm).

Preoperative assessment of T-stage

US and histopathology assessments (Table 1) displayed a 64% (61/96) rate of diagnostic agreement. The κ coefficient for T-staging overall was 0.48 (95% CI 0.35–0.62; $p < 0.001$), indicating a moderate capacity to reproduce histopathologic T-stage assignment via US. However, Spearman's rank correlation coefficient was 0.798

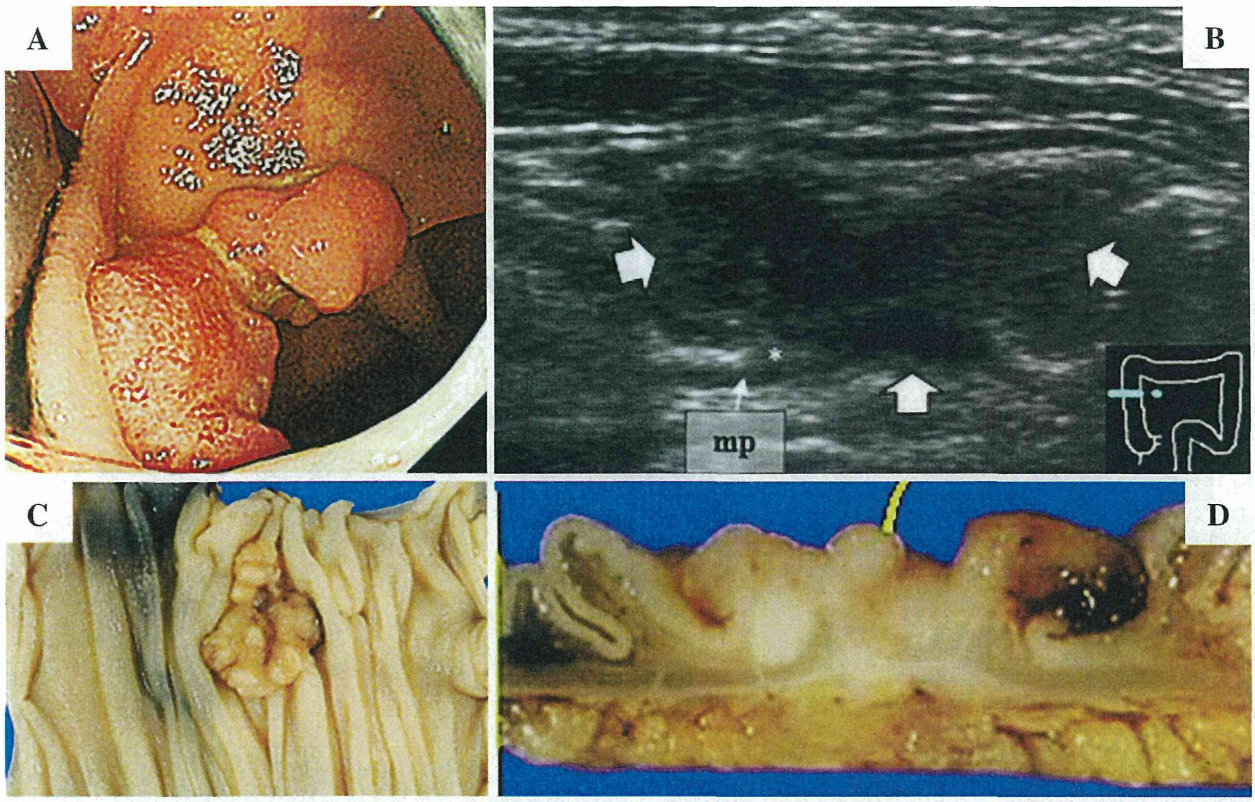

Fig. 4. Representative sonograph of stage T2 tumor. **A** Type 2 tumor of ascending colon on colonoscopy. **B** Hypoechoic tumor as mural thickening (larger white arrows) on transabdominal US. Muscularis propria (MP, smaller white arrow) distinguishable as hypoechoic layer. Submucosa appears as hyperechoic layer (*) above MP. Stage T2 assigned based on completely interrupted submucosal layer. **C** and **D** Resected tumor shown, confirmed as stage T2 by histopathology.

($p < 0.001$), signaling high-level agreement. Sensitivity and PPV of US were relatively low at any T-stage level (respective ranges: 47–71% and 36–75%); but specificity, NPV, and accuracy were relatively high at stages Tis, T1, and T2 (all >90%). Nonetheless, specificity, NPV, and accuracy at stages T3 and T4 reflected relatively low performance (all <80%), particularly in terms of distinguishing stages T3 and T4.

Comparison of US and conventional CT

Tumor detection rates of US and conventional CT and the accuracy of each method in differentiating stages T3 and T4 are shown (Table 2). Tumor detection by US (98%) significantly exceeded that of conventional CT (79% [77/98]; $p < 0.001$), differing significantly at T1 stage (89% vs. 26%, $p < 0.001$) or at tumor size <30 mm, (94% vs. 48%, $p < 0.001$). US and conventional CT performed similarly with respect to differentiating stages T3 and T4, (Table 2).

Three-tier approach to ultrasonographic T-stage determination

In our view, a 64% rate of diagnostic agreement is not helpful clinically, especially given the extremely low accuracy (<80%) of diagnosing T3 and T4 (vs. lesser stages). Based on extent of intestinal mural involvement (as shown in Table 1), risk of lymph node metastasis according to data in Japanese guidelines (Tis, 0%; T1, 9.1%; T2, 21.0%; T3, 42.3%; T4a, 62%; and T4b, 53.7%) [13], and the fact that MP was relatively thick and thus recognizable, we subsequently stratified tumors as follows for diagnostic US purposes: Tis/T1 (below MP), T2 (within MP), and T3/T4 (beyond MP). Accordingly, diagnostic agreement rose to 89% (85/96), with a κ coefficient of 0.77 (95% CI 0.64–0.90; $p < 0.001$), indicating good agreement (Table 3). Likewise, the correlation coefficient climbed to 0.887 ($p < 0.001$), indicating a particularly strong correlation.

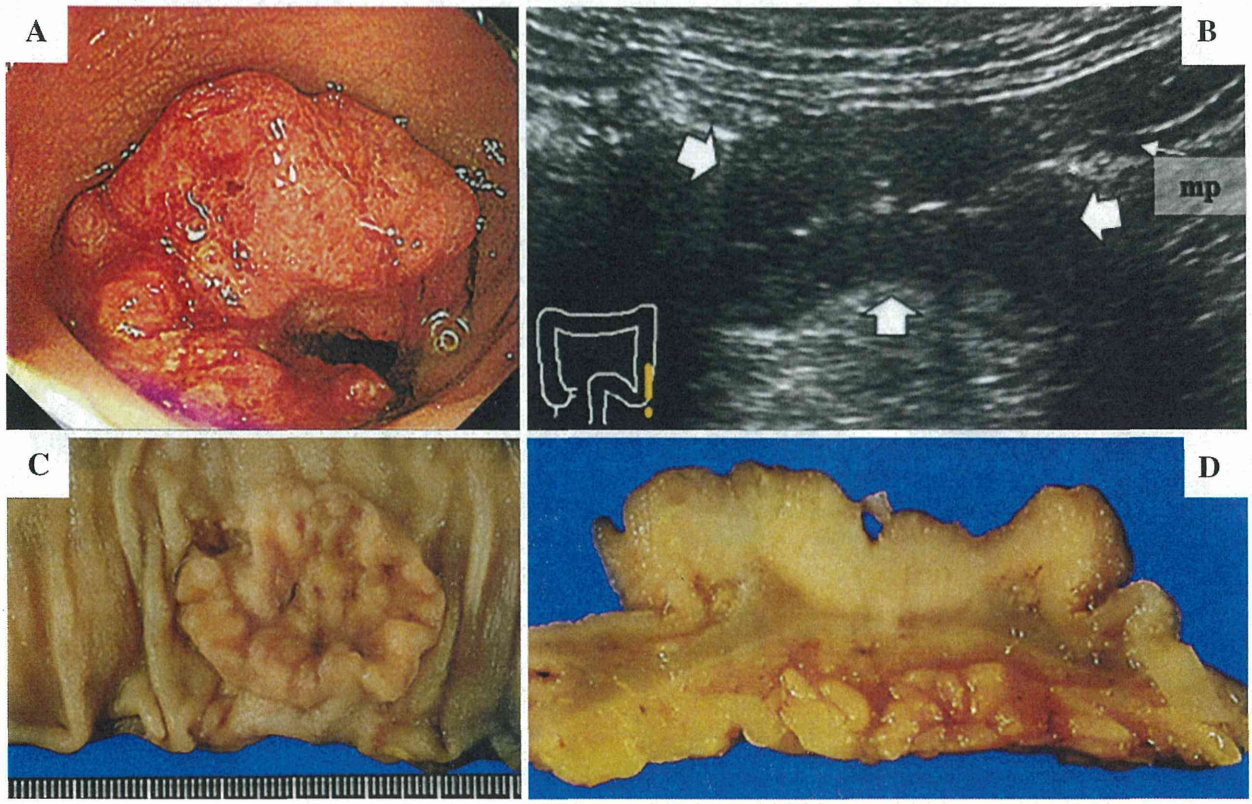

Fig. 5. Representative sonograph of stage T3 tumor. **A** Type 2 tumor of colon at SD junction on colonoscopy. **B** Hypoechoic tumor as mural thickening (*larger white arrows*) on transabdominal US. Muscularis propria (*MP, smaller white arrow*) distinguishable as hypoechoic layer. Submucosa appears as hyperechoic layer (*) above MP. Stage T3 assigned based on completely interrupted MP layer. **C** and **D** Resected tumor shown, confirmed as stage T3 by histopathology.

Results of ultrasonographic diagnostics by location

Diagnostic agreement for tumors at various locations in the colon is summarized in Table 4. T-stage agreement by layer was moderate to relatively high (60–76%), except for poor agreement (44%) at cecum. However, diagnostic agreement improved at all locations when stratified as above (78–100%).

Analysis of clinical factors potentially impacting diagnostic ultrasonography

Univariate analysis was applied to analyze whether patient demographics or tumor characteristics impacted agreement between US and histopathology. For both methods utilized, we found no significant differences in accuracy of T-stage determination that were related to gender, age, body mass index (BMI), preoperative values (including hemoglobin, albumin, and C-reactive protein), tumor size, thickness of bowel wall, tumor differentiation, or presence of distant metastases (Table 5).

Discussion

Due to the poor performance of older machines and interference by intestinal gas, use of US to evaluate colonic tumors has been considered difficult. Thus, its application in the screening or investigation of colon cancer has been limited. For our purposes, we first located the thin and exceedingly low echoic colonic wall (with its characteristic haustration), which then facilitated identification of high echoic intestinal gas. Cancerous lesions ultimately were confirmed by more than two cross sectional and/or color Doppler studies. To examine structural layers of bowel wall, high-frequency probes (center frequency >6 MHz) were used. In this way, nearly all colonic tumors established by colonoscopy (98%; 96/98) were detected by US as well. Each of two tumors that escaped detection by US were stage T1 lesions <15 mm in size, located at splenic flexure of descending colon. Because the splenic flexure is situated deep within the abdomen and is obscured by the ribs, this location may not be amenable to diagnostic US. Otherwise, the capacity of US to detect colonic tumors

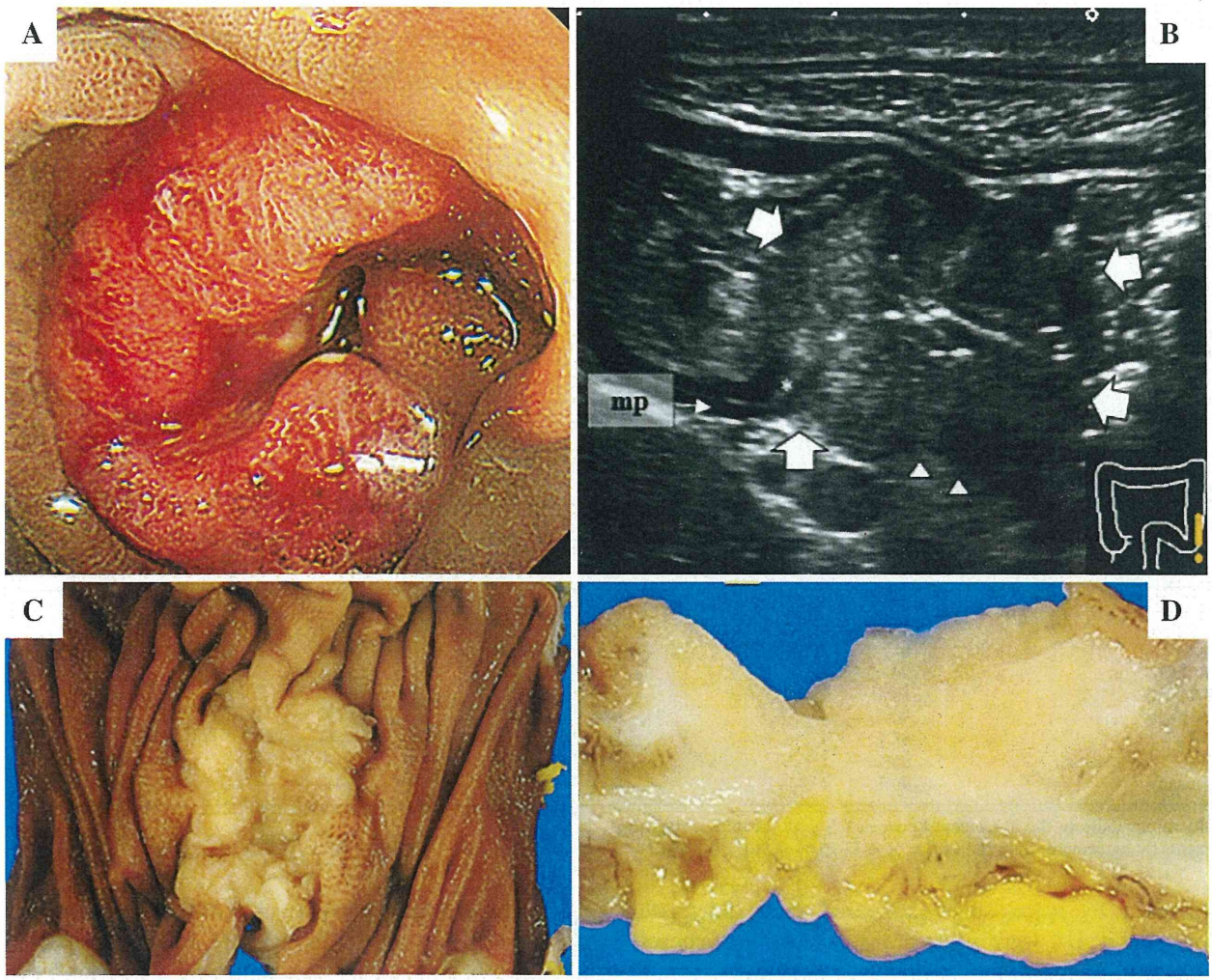

Fig. 6. Representative sonograph of stage T4 tumor. **A** Type 0-Isp tumor of colon at SD junction on colonoscopy. **B** Hypoechoic tumor as mural thickening (*larger white arrows*) on transabdominal US. Muscularis propria (*MP, smaller white arrows*) distinguishable as hypoechoic layer. Submucosa appears as hyperechoic layer (*) above MP. Stage T4 assigned based on unclear subserosal border (arrowheads). **C** and **D** Resected tumor shown, confirmed as stage T4 by histopathology.

Table 1. Agreement in depth of tumor infiltration (T-stage) by intestinal mural layer

US-stage	Staged by histopathology					
	Tis	T1	T2	T3	T4	Total (*n*)
Tis	**5**	3				8
T1	1	**12**	2	1		16
T2	1	2	**4**	4		11
T3			1	**31**	10	42
T4				10	**9**	19
Total (*n*)	7	17	7	46	19	96
Sensitivity	71%	71%	57%	67%	47%	
Specificity	98%	95%	92%	78%	87%	
PPV	63%	75%	36%	74%	47%	
NPV	98%	94%	96%	72%	87%	
Accuracy	95%	91%	90%	73%	79%	

Bold values indicate the agreement between US and pathologic diagnosis
Diagnostic agreement: 64% (61/96), $\kappa = 0.48$ (0.35–0.62), $p < 0.001$